Material Temperature Dependence of the Retention and Sputtering Yield of Single-Crystal Graphite under Hydrogen Plasma Irradiation*)

Seiki SAITO, Masayuki TOKITANI[1)] and Hiroaki NAKAMURA[1)]

National Institute of Technology, Kushiro College, 2-32-1 Otanoshike-Nishi, Kushiro 084-0916, Japan
[1)]*National Institute for Fusion Science, 322-6 Oroshi-cho, Toki, Gifu 509-5292, Japan*

(Received 25 November 2014 / Accepted 31 March 2015)

Carbon is a candidate material for divertor plates in nuclear fusion devices. To investigate the erosion and hydrogen retention in carbon at the atomic scale, we performed molecular simulations of hydrogen injection into single-crystal graphite considering the thermal vibration of the target atoms, the diffusion of incident atoms in the target material, and the structural relaxation of the target material. Then, the dependence of hydrogen retention and sputtering yield on material temperature was investigated in detail.

© *2015 The Japan Society of Plasma Science and Nuclear Fusion Research*

Keywords: plasma-material interaction, graphite, hydrogen plasma, molecular simulation, binary collision approximation

DOI: 10.1585/pfr.10.3403075

1. Introduction

The divertor plates in nuclear fusion devices are exposed to energetic hydrogen plasmas. Under hydrogen plasma irradiation, surface erosion and hydrogen retention are observed on the surface of the divertor plates. The erosion of materials generates impurities owing to physical and chemical sputtering. Impurities decrease the plasma temperature when they are ionized in the fusion plasma. Tritium inventory in the divertor plates is also an important issue because it may lead to the significant reduction of the lifetime of the materials. For the steady-state operation of nuclear fusion devices, it is important to understand the elementary processes of the sputtering of divertor plates and hydrogen retention under plasma irradiation at the atomic scale.

Carbon is a candidate material for divertor plates although tungsten has attracted considerable attention in recent years. For example, the divertor plates of the Large Helical Device at the National Institute for Fusion Science in Japan are composed of graphite. To investigate the erosion and hydrogen retention in graphite at the atomic scale, we performed molecular simulations.

The process of plasma–material interaction is often investigated using the binary collision approximation (BCA)-based simulation code, for example, Atomic Collision in Amorphous Target (ACAT) [1], EDDY [2], ERO, and TRIM [3] codes. In a previous study, we extended ACAT to the Atomic Collision in Any structured Target (AC∀T) code to handle all structures of a target material, including monocrystals, polycrystals, crystals with defects, and amorphous phases [4]. In addition, the AC∀T code can treat the time evolution of target materials during plasma irradiation [5], the thermal vibration of the target atoms [6], the diffusion of incident atoms in the target materials, and the structural relaxation of target materials [7]. In this study, we perform BCA simulations of hydrogen injection into single-crystal graphite using the AC∀T code to investigate sputtering and hydrogen retention in graphite under hydrogen plasma irradiation. The sputtering yield and retention strongly depend on material temperature; therefore, we investigate the dependence of these processes on material temperature in detail.

2. Simulation Method [5–8]

The AC∀T code solves motions of atoms based on BCA and the Moliere approximation to the Thomas–Fermi potential [9, 10]. In addition to the BCA-based simulation, the thermal vibrations of target atoms, the diffusion of incident atoms, and the relaxation of target materials are calculated. In this section, the algorithm for these calculations is discussed.

The AC∀T code first stores the initial positions of carbon atoms as perfect single-crystal graphite. Following hydrogen injection, the stored positions of the carbon atoms are overwritten. The stop positions of the incident hydrogen atoms are also stored at each injection. The positions of the target atoms in each binary collision are temporarily displaced from the stored positions of the collision target using the distances Δx, Δy and Δz distributed by

$$f(\Delta x, \Delta y, \Delta z) = \sqrt{\frac{k_x k_y k_z \beta^3}{8\pi^3}} \mathrm{e}^{-\beta(k_x \Delta x^2 + k_y \Delta y^2 + k_z \Delta z^2)/2},$$

author's e-mail: saitos@kushiro-ct.ac.jp

*) This article is based on the presentation at the 24th International Toki Conference (ITC24).

© 2015 The Japan Society of Plasma Science and Nuclear Fusion Research

where k_x, k_y and k_z are spring constants. $\beta = k_B^{-1}T^{-1}$ where k_B is the Boltzmann constant, and T is the material temperature. Spring constants k_x, k_y and k_z depend on the bonding state of the collision target and are determined by molecular dynamics simulation. For more details regarding the treatment of thermal vibrations by the AC∀T code, see Ref. [6].

The following one-dimensional diffusion equation along the depth direction (z-axis) is used to model the diffusion of retained hydrogen atoms

$$\frac{\partial n}{\partial t} = D\frac{\partial^2 n}{\partial z^2},$$

where D is the diffusion coefficient, z is the depth from the surface, and $n(t, z)$ is the density distribution of the retained hydrogen atoms at time t. The initial density distribution $n(0, z)$ is calculated using the positions of hydrogen atoms in the target material. The boundary conditions are set to $n(t, 0) = n(t, z_{max}) = 0$, where z_{max} is the bottom of the target material. To minimize computation time, the diffusion calculations are performed after completing 100 injections. The density distribution after 100 injections $n(\tau, z)$ is calculated from the initial distribution $n(0, z)$ by integrating the diffusion equation. The physical time for 100 injections is $\tau = 100/(S \times F)$, where S is the surface of the target material and F is the incident flux. The AC∀T code approximates the diffusion coefficient as constant although it depends on the material's structure. Other simulation codes such as TMAP7 consider the surface recombination and diffusant trapping at trapping sites. This will be investigated in future studies, as we plan to add these calculations to the AC∀T code.

Atoms of the target material move toward stable positions because of the interatomic potential. To consider the structural relaxation of the target materials, the interatomic potential $U(\{\boldsymbol{r}\})$ is introduced in our simulations, where $\{\boldsymbol{r}\}$ denotes the set of positions of all atoms in the system. The relaxed structure of the target materials is obtained by minimizing the potential energy $U(\{\boldsymbol{r}\})$. In the carbon–hydrogen system, we use Brenner's potential [11] for $U(\{\boldsymbol{r}\})$.

$$U = \sum_{i,j>i}\left[V^{R}_{[ij]}(r_{ij}) - \bar{b}_{ij}(\{\boldsymbol{r}\})V^{A}_{[ij]}(r_{ij})\right],$$

where r_{ij} is the distance between the i-th and j-th atoms. Functions $V^{R}_{[ij]}$ and $V^{A}_{[ij]}$ represent repulsion and attraction, respectively, and $\bar{b}_{ij}$ generates a many-body force. Similar to the diffusion calculation, we calculate the structural relaxation at every 100 injections. For more details regarding the treatment of diffusion and relaxation with the AC∀T code, see Ref. [7].

3. Simulation Model

We simulate hydrogen injection into single-crystal graphite using the AC∀T code. The dimensions of the target material are 30.1 Å × 26.0 Å × 334.8 Å. The z-axis of the simulation box is set parallel to the edge of the target material with a length of 334.8 Å. Periodic boundary conditions are used in the x- and y-directions. The temperature

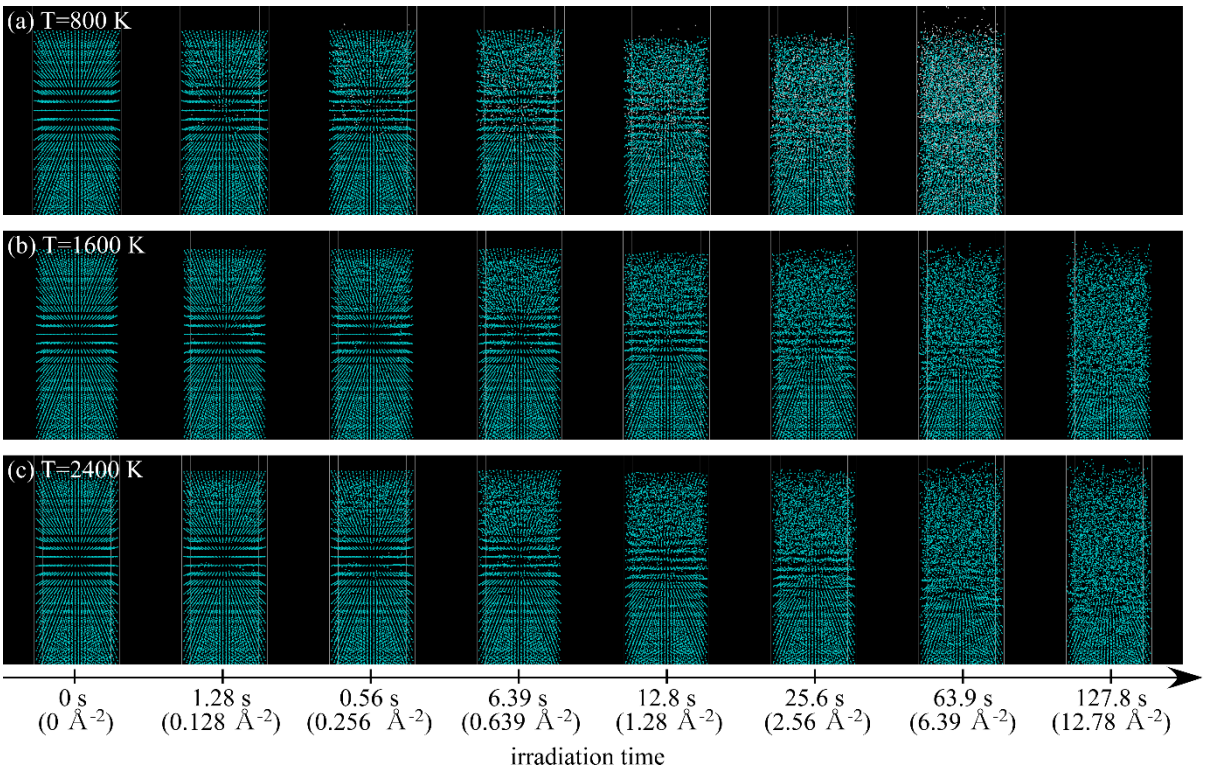

Fig. 1 Time evolution of target material near surface when material temperature is (a) 800 K, (b) 1600 K, (c) 2400 K. Green and white dots denote carbon and hydrogen atoms, respectively.

of the target material is set to 800 K, 1600 K, and 2400 K. Ten thousand hydrogen atoms are injected one-by-one into the target material. The incident energy of the hydrogen atoms is fixed at 100 eV. The incident angle is set parallel to the z-axis, i.e., perpendicular to the (0001) surface. The x- and y-coordinates of the starting positions of hydrogen atoms are randomly set.

The diffusion coefficient D is calculated using the following equation:

$$D = D_0 e^{-Q/(k_B T)},$$

where T is the material temperature. $D_0 = 1.85 \times 10^{-4}$ Å^2/ns and $Q = 0.66$ eV are obtained by fitting the data for the hydrogen diffusion coefficient in carbon in Ref. [12]. At 800 K, 1600 K, and 2400 K, the diffusion coefficient D is 1.29×10^{-8} Å^2/ns, 1.54×10^{-6} Å^2/ns, and 7.61×10^{-6} Å^2/ns, respectively. The incident flux F is set to 1.0×10^{-10} Å^{-2}ns^{-1}. Therefore, the interval between injections is 12.8 ms.

4. Results

Figure 1 shows the time evolution of the target material near the surface at (a) 800 K, (b) 1600 K, (c) 2400 K. Clearly, the crystalline structure of graphite is destroyed with increasing irradiation time. Compared with the results at 1600 K or 2400 K, many hydrogen atoms are retained near the material surface at 800 K because the corresponding diffusion coefficient is low. At 800 K, the simulation is aborted when the irradiation time t is 65.2 s because of the error associated with the high condensation of hydrogen atoms. At 1600 K and 2400 K, most of the incident hydrogen atoms are evacuated from the surface of the target material by diffusion.

Figure 2 (a) shows the time evolution of hydrogen density. The density quickly saturates at low values at high T. Figure 2 (b) shows the depth profile of hydrogen density at $t = 6.4$ s and $t = 64.0$ s. Hydrogen is distributed to almost the entire area of the target material at 1600 K and 2400 K, whereas hydrogen is unevenly distributed near the surface at 800 K. At 1600 K and 2400 K, hydrogen density n peaks near the half-depth of the target material because of the boundary condition $n(t, 0) = n(t, z_{max}) = 0$.

Figure 3 shows the time evolution of the generation rate of (a) sp^2, (b) 1-bond, (c) sp, and (d) sp^3 carbon atoms. Here, 1-bond denotes carbon atoms or hydrogen atoms that have only one covalent bond. As irradiation time increases, sp^2 carbon atoms change to other bonding states, such as 1-bond, sp, and sp^3. At $T = 800$ K, the generation of 1-bonds and sp^3 bonds is significant. We consider that the 1-bonds and sp^3 bonds are generated because many hydrogen atoms bond with sp^2 carbon atoms near the surface.

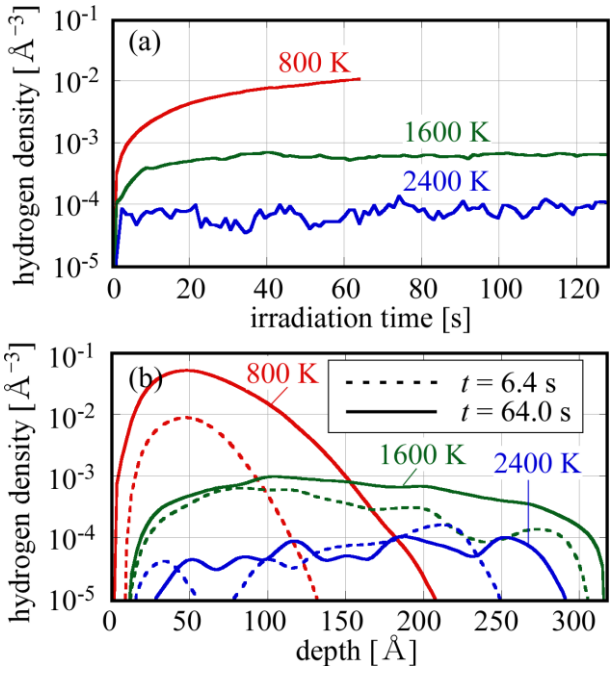

Fig. 2 (a) Time evolution and (b) depth profile of hydrogen density.

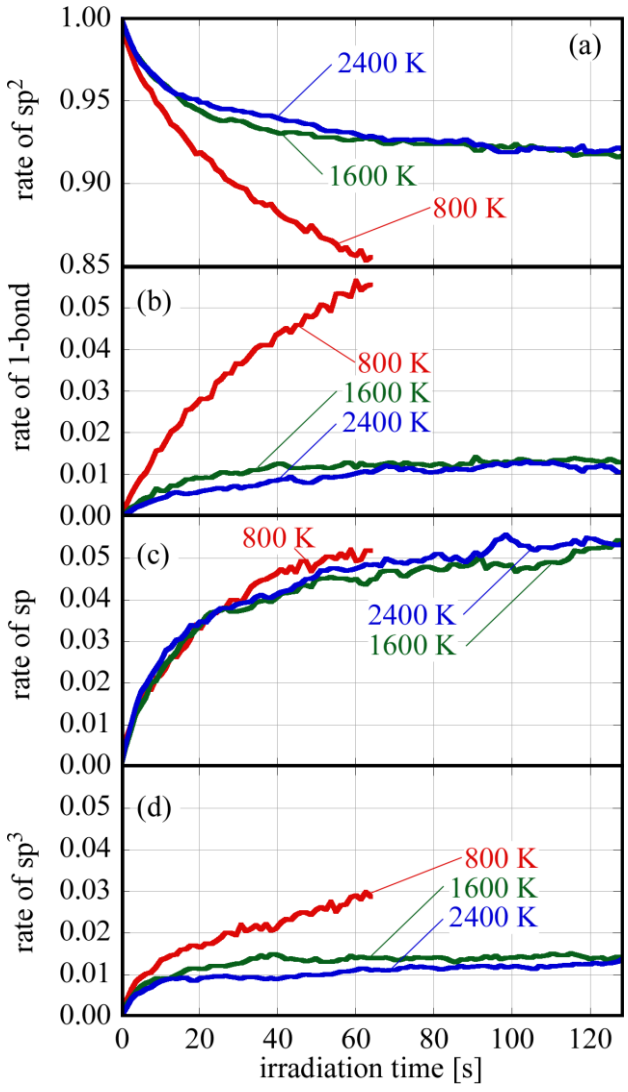

Fig. 3 Time evolution of the rate of (a) sp^2, (b) 1-bond, (c) sp, and (d) sp^3.

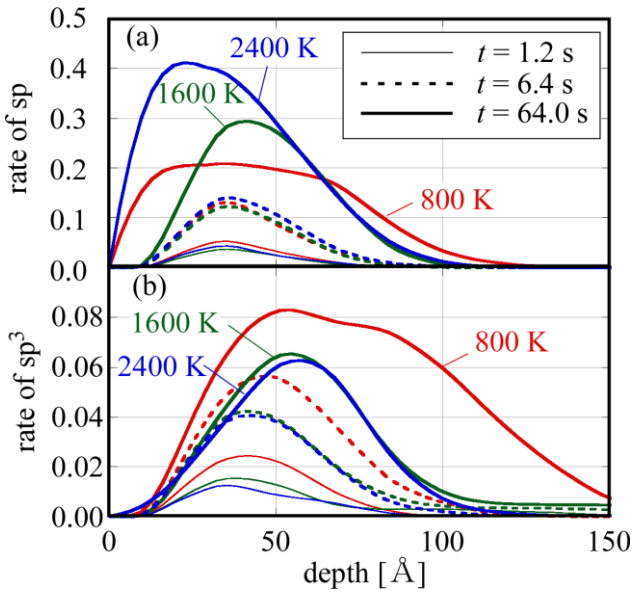

Fig. 4 Depth profile of rate of (a) sp, (b) sp^3.

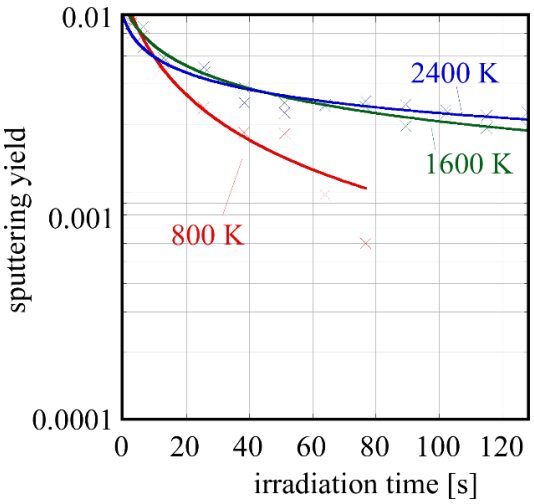

Fig. 5 Time evolution of sputtering yields for different material temperature.

Figure 4 (a) shows the depth profile of the generation rate of sp carbon atoms. The rate of sp carbon atoms decreases with T. Three sp carbons are generated when a sp^2 carbon atom in a graphene sheet recoils. Therefore, we consider that the rate of sp decreases at 800 K because many hydrogen atoms bond with sp carbon atoms near the surface. Figure 4 (b) shows the depth profile of the rate of sp^3 carbon atoms. The rate of sp^3 carbon atoms increases as Tdecreases. This explains why many hydrogen atoms bond with sp^2 carbon atoms at 800 K, as mentioned above. Comparing Figs. 4 (a) and 4 (b), we see that the depth where the sp^3 rate is maximum is deeper than that where the sp rate is maximum. We consider that the sp^3 carbon atoms are generated when recoil atoms or incident hydrogen atoms stop and bond with sp^2 carbon atoms, although sp carbon atoms are generated at the positions target atoms recoil.

Figure 5 shows the time evolution of sputtering yield for different material temperatures. Sputtering yields are calculated using "independent" simulation for each target material calculated by "cumulative" simulation. For detail regarding the "independent" and "cumulative" simulations, see Ref. [6]. Sputtering yields decrease with increasing irradiation time. The yield at 800 K is smaller than that at 1600 K and 2400 K because more incident energy is consumed to eject the retained hydrogen atoms from the material at 800 K.

5. Summary

The BCA simulation of hydrogen injection into single-crystal graphite is conducted using the ACΨT code. Then, the dependence of the sputtering yield and retention on the material temperature are investigated.

Density quickly saturates at low values when T is high. At T = 1600 K and 2400 K, most of the incident hydrogen atoms are evacuated from the surface of the target material by diffusion. As irradiation time increases, sp^2 carbon changes to other bonding states, such as 1-bond, sp, and sp^3. With decreasing T, the generation rate of sp carbon atoms decreases and that of sp^3 carbon atoms increases. The sputtering yield at 800 K is smaller than that at 1600 K and 2400 K.

Acknowledgements

Numerical simulations were conducted using the Plasma Simulator at the National Institute for Fusion Science, Japan. This study was supported by the NIFS Collaborative Research Programs (NIFS14KNTS030 and NIFS14KNTS028) and a Grant-in-Aid for Young Scientists (B) (No. 26790065) from the Ministry of Education, Culture, Sports, Science, and Technology, Japan.

[1] Y. Yamamura and Y. Mizuno, Inst. Plasma Phys. Nagoya University, IPPJ-AM-40 (1985).
[2] K. Ohya and R. Kawakami, J. Appl. Phys. **40**, 5424 (2001).
[3] J.P. Biersack and W. Eckstein, Appl. Phys. **A73**, 34 (1984).
[4] A. Takayama, S. Saito, A.M. Ito, T. Kenmotsu and H. Nakamura, Jpn. J. Appl. Phys. **50**, 01AB03 (2011).
[5] S. Saito, A. Takayama, A.M. Ito and H. Nakamura, Proc. 30th JSST Annual Conference, 197 (2011).
[6] S. Saito, A. Takayama, A.M. Ito and H. Nakamura, Proc. 31st JSST Annual Conference, 46 (2012).
[7] S. Saito, M. Tokitani and H. Nakamura, Comm. Computer Info. Sci. **474**, 176 (2014).
[8] S. Saito, A.M. Ito, A. Kenmotsu and H. Nakamura, Progress in Nuclear Science and Technology **2**, 44 (2011).
[9] G. Moliere, Naturforsch. **2A**, 133 (1947).
[10] W. Eckstein, *Computer Simulations of Ion-Solid Interactions* (Springer-Verlag, Berlin, 1991).
[11] D.W. Brenner, O.A. Shenderova, J.A. Harrison, S.J. Stuart, B. Ni and S.B. Sinnott, J. Phys. Condens. Matter **14**, 783 (2002).
[12] T. Tanabe and Y. Watanabe, J. Nucl. Mater. **179-181**, 231 (1991).